

Este artículo puede ser usado únicamente para uso personal o académico. Cualquier otro uso requiere permiso del autor o editor.

El siguiente artículo fue publicado en *Revista Mexicana de Física*, 63(2): 117-123, (2017); y lo puede consultar en <https://rmf.smf.mx/>

## Experimental multi-scroll attractor driven by switched systems

I. Campos-Cantón<sup>a</sup>, E. Campos-Cantón<sup>b</sup>, S. González-Bautista<sup>a</sup> and R.E. Balderas-Navarro<sup>a</sup>

<sup>a</sup>*Instituto de Investigación en Comunicación Óptica (IICO), Facultad de Ciencias,  
Universidad Autónoma de San Luis Potosí.*

*Alvaro Obregón 64, 78000 San Luis Potosí, SLP, México.*

*email: icampos@ciencias.uaslp.mx*

<sup>b</sup>*Div. Mat. Aplicadas, IPICYT*

*Camino a la Presa San José 2055, 78216, SLP, SLP, México.*

Received 18 May 2016; accepted 6 December 2016

This article deals with an electronic implementation of a 3-D dynamical system that comprises multiple scrolls and is regarded as unstable dissipative system. Such a system is dissipative in one of its components but unstable in the other two. The proposed electronic circuit is implemented with resistors, capacitors and comparators and has the capability to generate two or three scrolls

*Keywords:* Phase portrait; Analog electronic; Differential equations; Operational Amplifier.

Este artículo trata de la instrumentación de un sistema dinámico 3-D que puede presentar múltiples enrollados, cual se ha denominado sistema disipativo inestable. Este sistema es disipativo en uno de sus componentes pero inestable en los otros dos. El circuito eléctrico propuesto esta constituido por resistencias, capacitores y comparadores. Este circuito es capaz de generar dos y tres enrollados.

*Descriptor:* Retrato de fase; electrónica analógica; ecuaciones diferenciales; amplificadores operacionales.

PACS: 02.10.Yn; 02.30.Hq; 02.10.Ab; 84.30.Sk; 84.30.Le

### 1. Introduction

In the last two decades, theoretical design of different kind of electronic circuits based on chaos have been a central subject. In this regard, the design of multi-scroll chaotic attractor is a challenging issue. Therefore, there are different choices concerning the implementation of chaotic circuits and one of them is the synthesis of electronic circuits with the capability of generating multi-scroll chaotic attractors. One idea is to modify a system that originally produces double-scroll attractors in such a way that multi-scrolls arise; as for example in the Chua and Lorenz systems [1-4]. As a matter of fact, Suykens and Vandewalle introduced several methods for generating n-scroll chaotic attractors using simple circuits [5,6]. Likewise, Yalcin and his colleagues [7] also reported work on multi-scroll chaotic attractors. Therefore, one of the main goals of chaotic systems is the search for alternatives to manipulate the number of scrolls in attractors without losing its dynamical behavior. Hitherto, different techniques are well established in the design of such systems, such as the modification of a simple sinusoidal oscillator [8], the improvement of existing chaotic systems [9-12] and through multi-fractal processes [13], among others.

In addition, new mechanisms of chaotic system generation have been reported from a theoretical viewpoint [14-17]. A simple technique is carried out in controlled systems by a switching control law [14], aimed at changing the switching control law in order to add further equilibria to the system, where each equilibrium point generates a scroll around it.

In this work, we propose an electronic implementation of a class of 3-D dynamical systems as already reported in Ref. 14. This class of systems is termed unstable dissipative

systems (UDS) because it is dissipative in one of its components while unstable in the other two. The UDS are constructed with a switching law in order to accomplish several multi-scroll strange attractors. The strange multi-scroll attractors appear as a result of the combination of several unstable “one-spiral” trajectories. Each of these trajectories lie around a saddle hyperbolic stationary point.

This work is organized as follows. In Sec. 1, both the UDS and the switching law are presented in order to produce multi-scroll chaotic attractors. The proposed electronic circuit of multi-scroll chaotic attractors using this approach is given in Sec. 2. Experimental results are given in Sec. 3, and conclusions are outlined in Sec. 4.

### 2. Unstable Dissipative Systems

We consider a linear system given by:

$$\dot{X} = AX, \quad (1)$$

where  $X = [x_1, \dots, x_n] \in \mathbb{R}^n$  is a state vector and  $A \in \mathbb{R}^{n \times n}$  is a linear operator. The equilibrium point of this system is located at the origin which is a saddle hyperbolic stationary point. Thus, one feature of matrix  $A$  relies on two generated manifolds, one stable  $E^s$  and another unstable  $E^u$ .

If the system given by Eq. 1 has a saddle equilibrium point responsible for unstable and stable manifolds and the sum of its eigenvalues is negative, then the system is called unstable dissipative system (UDS). In [14,15] two types of UDS in  $\mathbb{R}^3$  and two types of corresponding equilibria are defined.

**Definition 2.1** A system given by Eq. 1 in  $\mathbb{R}^3$  with eigenvalues  $\lambda_i$ ,  $i = 1, 2, 3$ , is said to be an UDS Type I, if

$\sum_{i=1}^3 \lambda_i < 0$  and one of its eigenvalues  $\lambda_i$  is both real and negative, and the other two are complex conjugate with a positive real part.

**Definition 2.2** A system given by Eq. 1 in  $\mathbb{R}^3$  with eigenvalues  $\lambda_i, i = 1, 2, 3$ , is said to be an UDS Type II, if  $\sum_{i=1}^3 \lambda_i < 0$  and one of its eigenvalues is both real and positive, and the other two are complex conjugate with a negative real part.

For the corresponding equilibria two types are defined accordingly. The above definitions imply that the UDS Type I is dissipative in one of its components but unstable in the other two, which both are oscillatory. The converse is the UDS Type II, which is dissipative and oscillatory in two of its components but unstable in the other one. These definitions work well for  $\mathbb{R}^3$  due to the fact that there is not ambiguity. However, for bigger dimensions  $\mathbb{R}^n$ , with  $n > 3$ , these type of UDS could be satisfied for both types of UDS, generating ambiguity. Therefore, a definition only for UDS systems is given as follows.

**Definition 2.3** Let a system defined by Eq. 1 in  $\mathbb{R}^n$  with eigenvalues  $\lambda_j, j = 1, \dots, n$  with none a pure imaginary eigenvalue. Each matrix  $A_i, i = 1, \dots, k$ , is said to be a dissipative and unstable system (UDS) if  $\sum_{j=1}^n \lambda_j < 0$  and there is at least one  $\lambda_j$  that is positive real or complex with positive real part.

The following proposition accounts for the types of behavior that are found in UDS system defined by Eq. 1.

**Proposition 2.1** Let system (1) be a UDS with an ordered set of eigenvalues  $\Lambda = \{\lambda_1 \dots \lambda_n\}$  and  $\lambda_1 \leq \lambda_2 \dots \leq \lambda_n$ . Then, the following statements are true:

- (a) The system has a stable manifold  $E^s = \text{span}\{\lambda_1 \dots \lambda_m\} \subset \mathbb{R}^n$  and one unstable  $E^u = \text{span}\{\lambda_{m+1} \dots \lambda_n\} \subset \mathbb{R}^n$ , with  $1 < m < n$ .
- (b) Any initial condition  $X_0 \in E^u$  generates an unstable trajectory; that is, an unbounded trajectory.
- (c) Any initial condition  $X_0 \in E^s$  generates a stable trajectory that converges to the equilibrium point.
- (d) The basin of attraction  $\mathfrak{B}$  is  $E^s \subset \mathbb{R}$ .

Proof: Let the eigenvalues  $\Lambda = \{\lambda_1 \dots \lambda_n\}$  have a set of corresponding eigenvectors  $\{v_1, \dots, v_n\}$ , which are linearly independent. Thus, there are  $m$  negative eigenvalues  $\lambda_1 \dots \lambda_m$  (real or complex with negative real part) accounting for the system to be dissipative. But there are  $n - m$  positive eigenvalues  $\lambda_{m+1} \dots \lambda_n$  (real or complex with positive real part) because of there are at least one pair of  $\lambda_j$  complex conjugate with positive real part. Then the stable and unstable subspaces of the linear system (1),  $E^s$  and  $E^u$ , are the linear subspaces spanned by  $\{v_1, \dots, v_m\}$  and  $\{v_{m+1}, \dots, v_n\}$ , respectively; i.e.,  $E^u = \text{span}\{\lambda_{m+1} \dots \lambda_n\} \subset \mathbb{R}^n$  with  $1 < m < n$ . This proves (a).

For statement (b), using the fundamental theorem for linear systems, the initial value problem of system (1) has a unique solution given by

$$x(t) = e^{At} X_0,$$

for a given  $X_0 \in E^u$ ; this unstable manifold is generated by positive real eigenvalues  $\lambda = a$ , and complex conjugate eigenvalues  $\lambda = a + ib$  with  $a, b \in \mathbb{R}$  and  $0 < a$ . Without loss of generality, the solution will be increasing according to  $e^{at}$ , when  $t \rightarrow \infty$  the solution  $|x(t)| \rightarrow \infty$ , thus generating unstable trajectories. In a similar way, for statement (c) the solution will be decreasing according to  $e^{at}$  due to  $a < 0$ , thus when  $t \rightarrow \infty$  the solution  $|x(t)|$  tends to the origin.

The spaces  $\mathbb{R}^n$  are the direct sum of subspaces  $E^s$  and  $E^u$ , then  $\mathbb{R}^n = E^s \oplus E^u$ . Therefore, as a consequence of (b) and (d), the basin of attraction  $\mathfrak{B}$  is  $E^s \subset \mathbb{R}$ , thus completing the proof. □

As already outlined in Ref. 14, we now consider a class of a switched system comprising affine piecewise linear systems given by:

$$\dot{X} = \begin{cases} A_1 X + B_1, & \text{for } X \in D_1, \\ \vdots \\ A_k X + B_k, & \text{for } X \in D_k, \end{cases} \quad (2)$$

where  $X = [x_1, \dots, x_n] \in \mathbb{R}^n$  is the state vector,  $B_i \in \mathbb{R}^n$  is a constant vectors,  $A_i \in \mathbb{R}^{n \times n}$  are linear operators,  $D_i$  are subspaces of  $\mathbb{R}^n$ , with  $i = 1, \dots, k$ . The equilibria of this system are located at  $X^* = -A_i^{-1} B_i$ , which are saddle hyperbolic stationary points. Thus, one feature of  $A_i$  is the existence of two generated manifolds: one stable  $E^s$  and the other unstable  $E^u$ .

Here, the goal is to find  $(A_i, B_i)$  subsystems that build up a switched system capable of generating periodic or chaotic oscillations in  $\mathbb{R}^3$ . We know that for a switched system to oscillate periodically or chaotically, it must contain at least two subsystems and if the system contains three or more subsystems, it can generate attractors with multiple scrolls.

Each subsystem  $A_i X + B_i$ , for  $X \in D_i$ , is denoted with the pair  $(A_i, B_i)$  and  $\mathbb{R}^n = \cup_{i=1}^k D_i$ , where  $X = [x_1, x_2, x_3]^T \in \mathbb{R}^3$  is the state variable,  $B = [b_1, b_2, b_3]^T \in \mathbb{R}^3$  stands for a real vector and each  $A_i \in \mathbb{R}^{3 \times 3}$  denotes a linear operator given as follows:

$$A = \begin{pmatrix} \alpha_{11} & \alpha_{12} & \alpha_{13} \\ \alpha_{21} & \alpha_{22} & \alpha_{23} \\ \alpha_{31} & \alpha_{32} & \alpha_{33} \end{pmatrix}. \quad (3)$$

As pointed out above, each matrix  $A_i$  is such that the system (2) is dissipative, which implies that the sum of eigenvalues are negative. In this way the characteristic polynomial of (3) is given by

$$g(\lambda) = \lambda^3 - \tau \lambda^2 + \gamma \lambda - \delta, \quad (4)$$

where  $\tau = Tr(A)$ ,  $\gamma = \alpha_{11}\alpha_{22} + \alpha_{11}\alpha_{33} + \alpha_{22}\alpha_{33} - \alpha_{13}\alpha_{31} + \alpha_{23}\alpha_{32} + \alpha_{12}\alpha_{21}$  and  $\delta = \det(A)$ . The classical Descartes' Rule of Signs is an useful tool to assess how

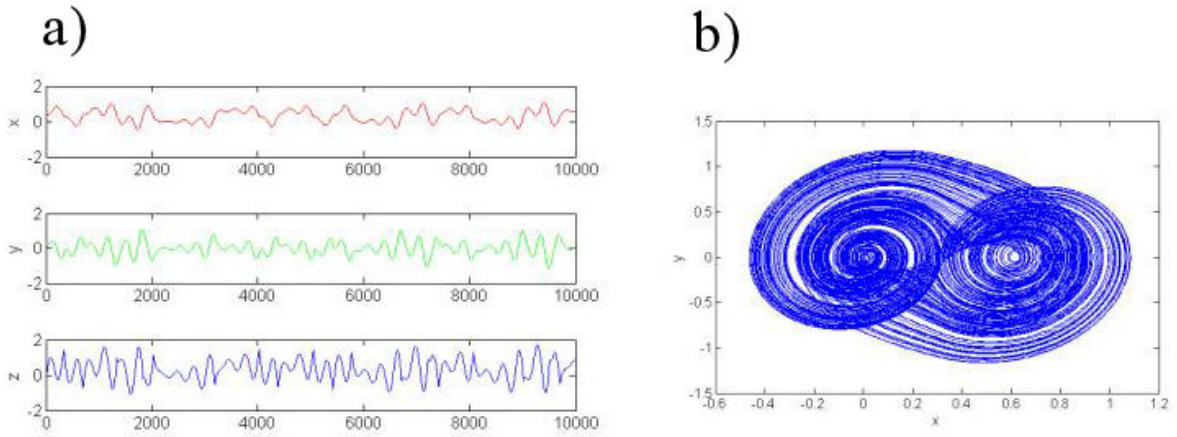


FIGURE 1. Two scrolls: a) states vs time, b) phase portrait  $X - Y$ .

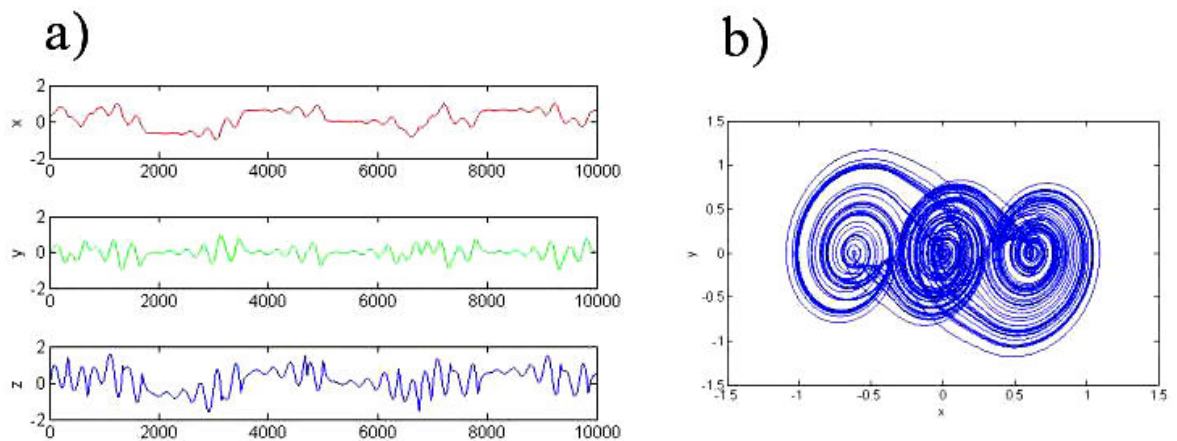


FIGURE 2. Three scrolls: a) states vs time and b) phase portrait  $X - Y$ .

many positive or negative roots one can expect from polynomial  $g(\lambda)$ . Then, if  $\tau < 0$ ,  $\delta < 0$ , and  $\gamma > 0$  imply two possibilities: (a) the roots of  $g(\lambda)$  are all real negative or (b)  $g(\lambda)$  has one real negative root and two complex roots with a positive real part. Since the first choice results in a stable equilibrium point, we are interested in case (b) because the component related to the negative real eigenvalue is attracting and the two complex eigenvalues are responsible for the steady outward slide.

**2.1. Two scrolls UDS**

If we chose  $\alpha_{11} = 0$ ,  $\alpha_{12} = 1$ ,  $\alpha_{13} = 0$ ,  $\alpha_{21} = -1$ ,  $\alpha_{22} = -0.2465$ ,  $\alpha_{23} = 1$ ,  $\alpha_{31} = -6.8438$ ,  $\alpha_{32} = -2.006$  and  $\alpha_{33} = -1.1102$  then the (b) condition of the previous paragraph is satisfied and the system given by Eq. (2) is UDS. The entries of  $B$  vector are:

$$B = \begin{cases} [0, 0, 5]^T, & \text{for } x \geq 0.3143, \\ [0, 0, 0]^T, & \text{other case.} \end{cases} \quad (5)$$

With these parameters, the equilibrium points are located at  $(0.6286, 0, 0.6286)$  and  $(0, 0, 0)$ , thus generating two scrolls as shown in Fig. 1.

**2.2. Three scrolls UDS**

If we add another equilibrium point, for example at  $(-0.6286, 0, -0.6286)$ , we generate three scrolls, and its  $B$  vector is (see Fig. 2):

$$B = \begin{cases} [0, 0, 5]^T, & \text{for } x \geq 0.3143, \\ [0, 0, 0]^T, & \text{for } -0.3143 < x < 0.3143, \\ [0, 0, -5]^T, & \text{for } x \leq -0.3143. \end{cases} \quad (6)$$

We are capable of generating more scrolls with this methodology if we add more equilibrium points as already stated in Ref. 14.

**3. Multi-scroll Electronic Circuit**

The proposed electronic circuit is based on the block diagram shown in Fig. 3, where  $v_x$  is a feedback to state  $v_z$ . The variables stated  $x$ ,  $y$ , and  $z$  in the above equations are the same role as the potentials  $v_x$ ,  $v_y$ , and  $v_z$  in our electronic model.

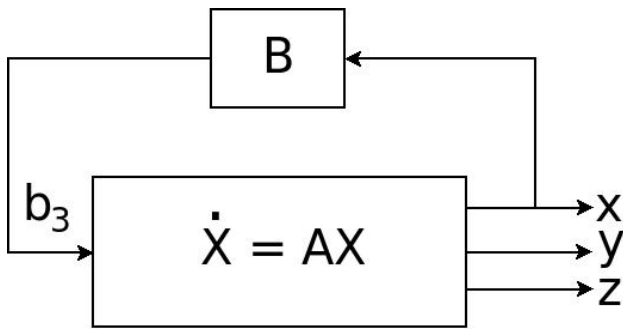


FIGURE 3. Block diagram of the proposed electronic circuit.

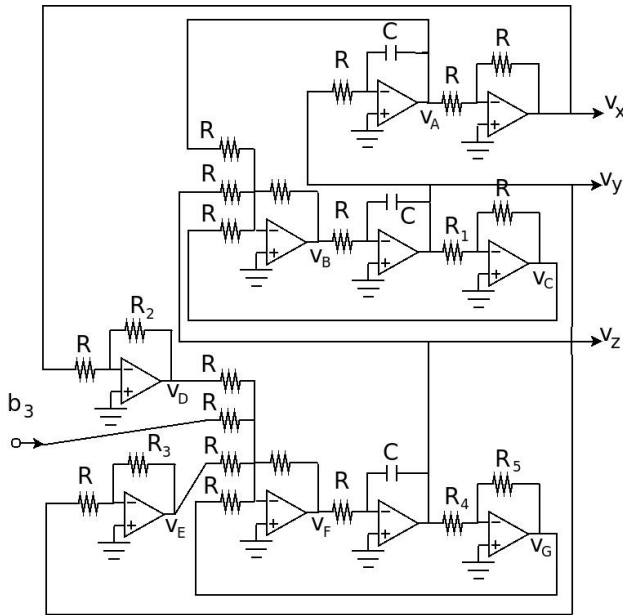


FIGURE 4. Electrical diagram of proposed electronic circuit, whit  $b_3$  as shown in Fig. 5.

The corresponding electronic diagram is implemented according to Fig. 4

Analyzing electronic circuit shown in Fig. 4, it is possible to get the following equations for node  $v_A$ :

$$v_A = -\frac{1}{RC} \int v_y dt, \tag{7}$$

$$v_x = -v_A;$$

then

$$\dot{v}_x = \frac{1}{RC} v_y. \tag{8}$$

For state  $v_y$ :

$$v_y = -\frac{1}{RC} \int v_B dt, \tag{9}$$

$$v_B = v_x - v_C - v_z,$$

$$v_C = -\frac{R}{R_1} v_y.$$

By manipulating Eq. (9), one obtains:

$$\dot{v}_y = -\frac{1}{RC} v_x - \frac{1}{R_1 C} v_y + \frac{1}{RC} v_z, \tag{10}$$

and the  $v_z$  state equation is given by:

$$v_z = -\frac{1}{RC} \int v_F dt,$$

$$v_F = -v_D - v_E - v_G - b_3,$$

$$v_D = -\frac{R_2}{R} v_x,$$

$$v_E = -\frac{R_3}{R} v_y,$$

$$v_G = -\frac{R_5}{R_4} v_z, \tag{11}$$

and therefore one obtains:

$$\dot{v}_z = -\frac{R_2}{R^2 C} v_x - \frac{R_3}{R^2 C} v_y - \frac{R_5}{R R_4 C} v_z + \frac{1}{RC} b_3. \tag{12}$$

Finally, from (8), (10) and (12), the  $A$  matrix and  $B$  vector are determined to be:

$$A = \begin{pmatrix} 0 & \frac{1}{RC} & 0 \\ -\frac{1}{RC} & -\frac{1}{RC} & \frac{1}{RC} \\ -\frac{R_2}{R^2 C} & -\frac{R_3}{R^2 C} & -\frac{R_5}{R R_4 C} \end{pmatrix}, \tag{13}$$

$$B = \begin{pmatrix} 0 \\ 0 \\ \frac{1}{RC} b_3 \end{pmatrix}. \tag{14}$$

According to Eq. (2), each matrix  $A_i = A$ . For vector  $B$ , the block diagram is shown in Fig. 5. Fig. 5a) shows the case in which two scrolls are generated. The circuit works as follows: when the state  $v_x$  is greater than 0.3 V, the comparator amplifier sets its output in high impedance and thus  $b_3$  goes to 5 V; in the other case, when  $v_x$  is less than 0.3 V the comparator amplifier output is grounded and thus  $b_3$  takes a 0 volts value. Thus, in this way  $b_3$  switched between 0 V and 5 V according to Eq. (5).

$$b_3 = \begin{cases} 5 \text{ V,} & \text{for } v_x \geq 0.3\text{V,} \\ 0 \text{ V,} & \text{other case;} \end{cases} \tag{15}$$

thus the  $B_i$  vectors are given by (14) and (15). According to Fig. 5b), the operation mode is as follows. The upper comparator operates in the same way as described for the case in Fig. 5a). The behavior of the lower comparator amplifier is as follows: if state  $v_x$  is less than -0.3 V, its output goes to high impedance (5 volts), otherwise takes 0 volts. The response of the two comparators and operational amplifiers is as follows: when state  $v_x$  is greater than 0.3 V,  $b_3$  is set to 5 V, or 0 volts if  $v_x$  lies between 0.3 V and -0.3 V; finally the response

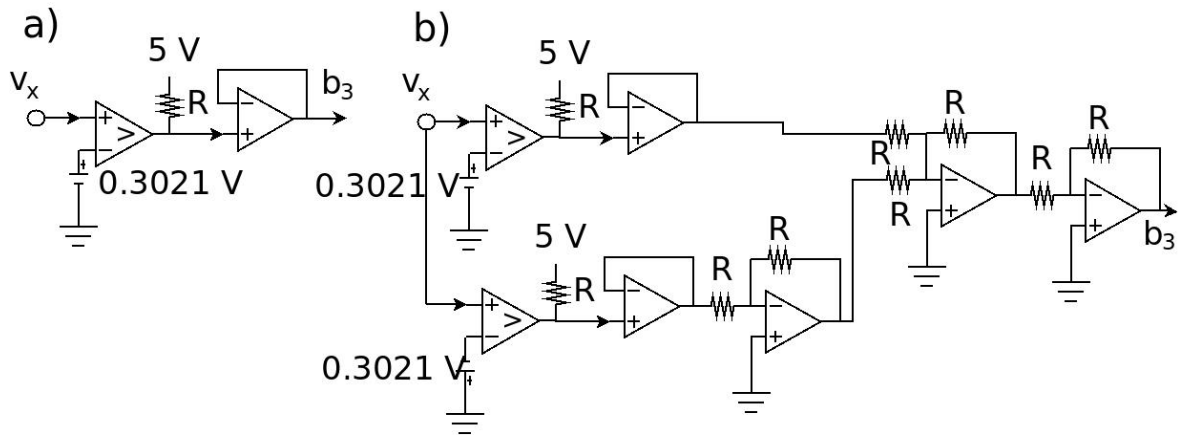


FIGURE 5. Electrical diagram for the  $B$  function as described in the text.

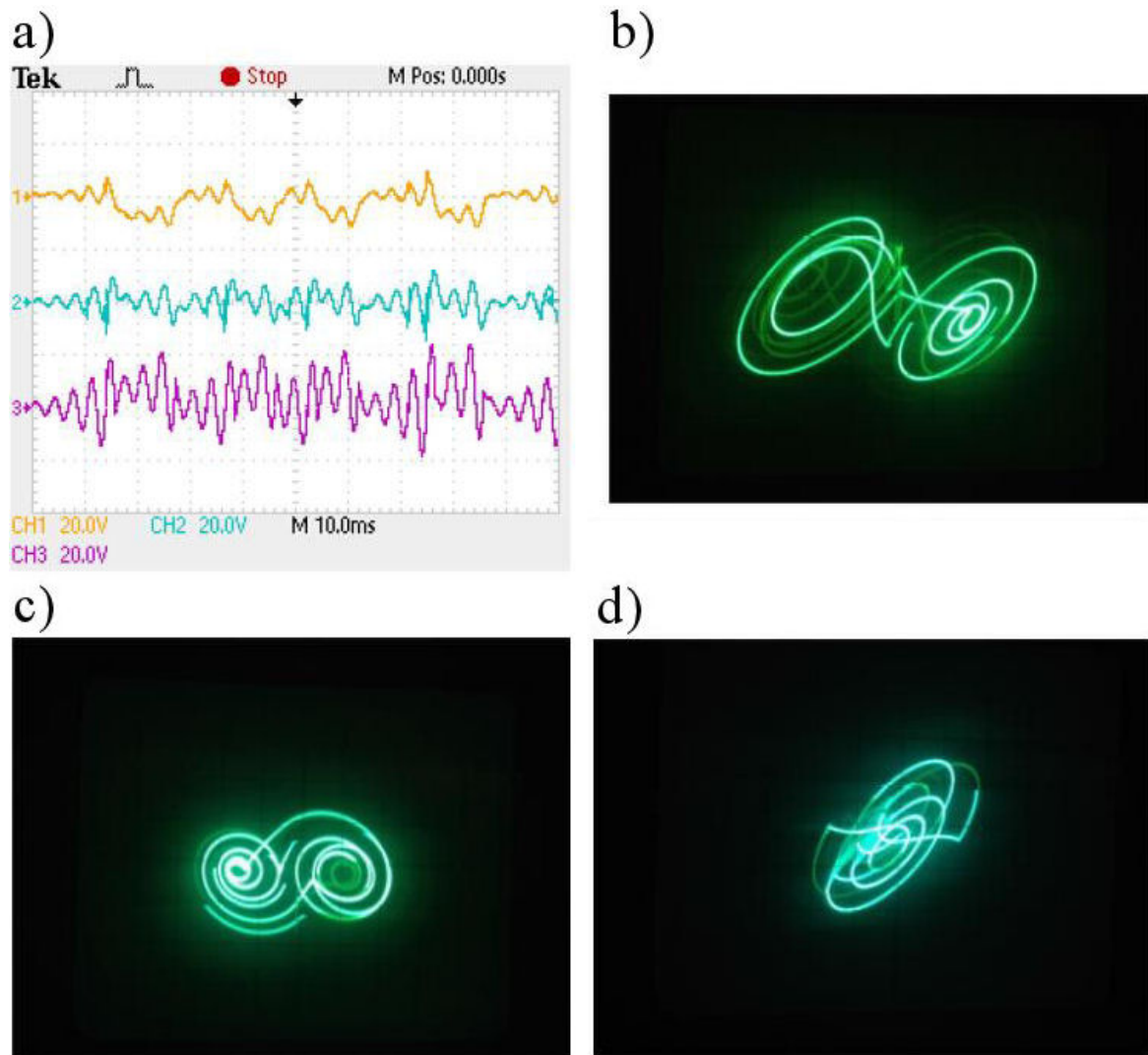


FIGURE 6. Double-scroll attractor: a) experimental time series of states. Different projections of the attractor on the b)  $v_x - v_z$  plane, c)  $v_x - v_y$  plane, and d)  $v_y - v_z$  plane.

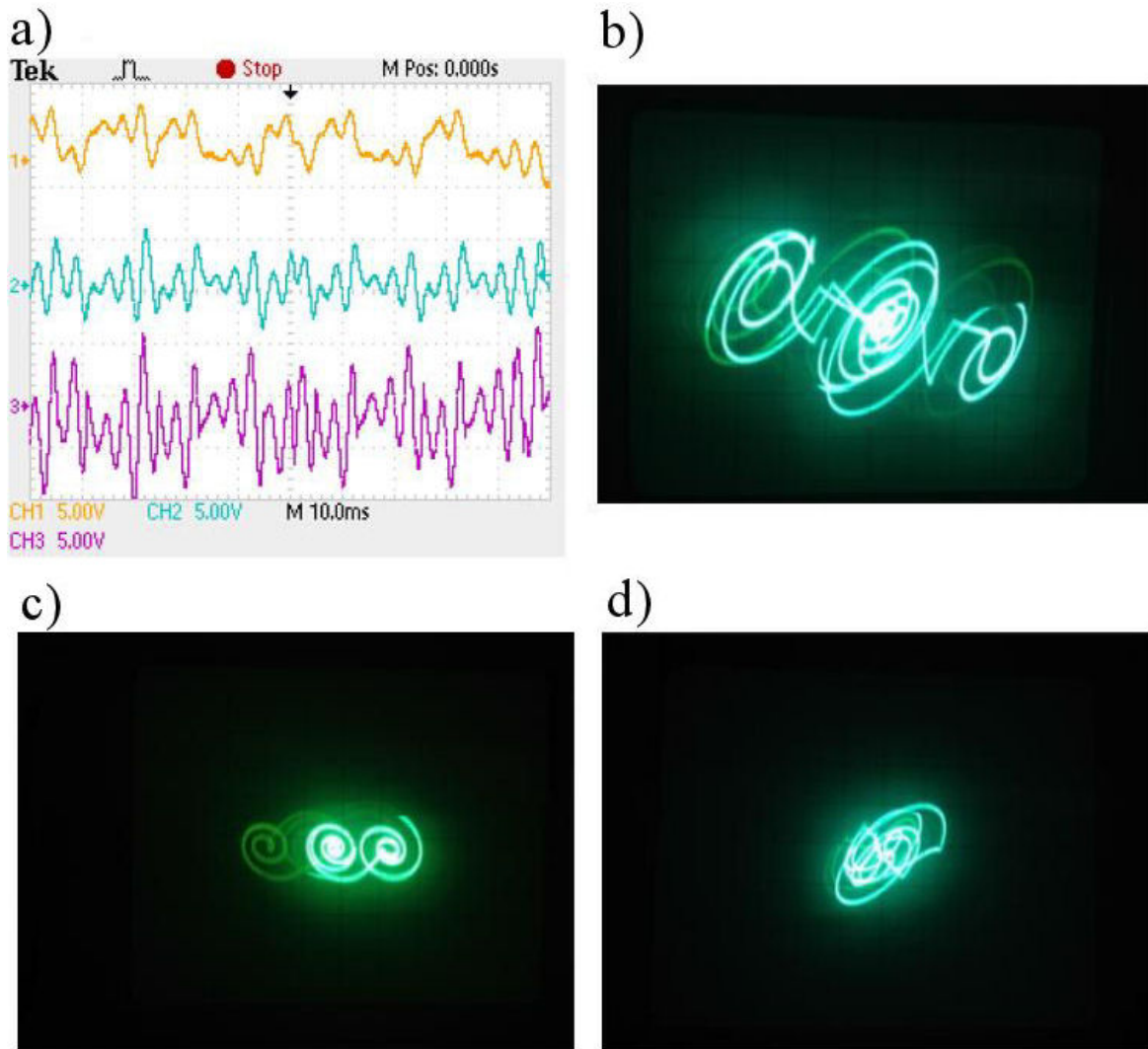


FIGURE 7. Triple-scroll attractor: a) experimental time series of states. Different projections of the attractor on the b)  $v_x - v_z$  plane, c)  $v_x - v_y$  plane, and d)  $v_y - v_z$  plane.

is -5 V if  $v_x$  attains a value less than -0.3 V. Accordingly, the response satisfies the following equation:

$$b_3 = \begin{cases} 5 \text{ V}, & \text{for } v_x \geq 0.3 \text{ V}, \\ 0 \text{ V}, & \text{for } -0.3 \text{ V} < v_x < 0.3 \text{ V}, \\ -5 \text{ V}, & \text{for } v_x \leq -0.3 \text{ V}; \end{cases} \quad (16)$$

where,  $B_i$  are given by Eqs. (14) and (16).

### 4. Experimental Results

The experimental results for a double-scroll attractor generated by the electronic circuit that corresponds to  $B_i$ , with  $i = 1, 2$  given by Fig. 5a) and described by Eq. (13), is shown in Fig. 6. The experimental time series are shown in Fig. 6a): the signal at the top corresponds to the  $v_x$  state, the middle signal is the  $v_y$  state, and the signal at the bottom is the  $v_z$  state. Different projections of the attractor are shown in

Fig. 6b) onto the  $v_x - v_z$  plane, c) onto the  $v_x - v_y$  plane and d) onto the  $v_y - v_z$  plane.

TABLE I. Electrical components used in the proposed circuit. See text for details.

Component	Value
$R$	1 K $\Omega$
$R_1$	4 K $\Omega$
$R_2$	7 K $\Omega$
$R_3$	3 K $\Omega$
$R_4$	4 K $\Omega$
$R_5$	4.4 K $\Omega$
$C$	1 $\mu$ F
Amplifier	TL081
Comparator	LM311

Figure 7 shows the experimental results for triple-scrolls attractor generated by the proposed circuits of Figs. 4 and 5b), which behavior is described by (16). The experimental time series are shown in Fig. 7a): the signal at the top corresponds to the  $v_x$  state, the middle signal is the  $v_y$  state, and the signal at the bottom is the  $v_z$  state. Different projections of the attractor are shown in Fig. 7b)  $v_x - v_z$  plane, c)  $v_x - v_y$  plane and d)  $v_y - v_z$  plane.

The components and values used to implement both, double-scroll and triple-scroll attractors, are given in Table I.

## 5. Conclusions

We have developed and implemented an electronic circuit based on what is called unstable dissipative system as proposed in Ref. 14, wherein the construction takes place

through PWL systems in a three dimensional space. The PWL system is given by the commutation of  $B_i$  vectors through one parameter, for which multiple scrolls are generated. The present work reports only double and triple scrolls but its generalization can be obtained in a similar way; to generate more scrolls in the proposed circuit, one has to modify vector  $B$ . In this way more equilibria are added to the system.

## Acknowledgments

S. González-Bautista is a master fellow of CONACYT (México) in the Graduate Program on Applied Science at IICO-UASLP.

E. Campos-Cantón acknowledges CONACYT (México) for the financial support through project No. 181002.

- 
1. J.A.K. Suykens and L.O. Chua, *Int. J. Electron. Commun.* **51** (1997) 131-138.
  2. R. Miranda and E. Stone, *Phys. Lett. A* **178** (1993) 105-113.
  3. E. Campos-Cantón, I. Campos-Cantón, J.S. González Salas and F. Cruz Ordaz, *Rev. Mex. de Fis.* **54** (2008) 411-415.
  4. B.C. Bao, Q.D. Li, N. Wang, and Q. Xu, *Chaos* **26** (2016) 043111.
  5. J.A.K. Suykens and J. Vandewalle, *IEE Proceedings-G* **138** (1991) 595-603.
  6. J.A.K. Suykens and J. Vandewalle, *IEEE Trans. Circuits Syst. I* **40** (1993) 861-867.
  7. M.E. Yalcin, J.A.K. Suykens, J. Vandewalle and S. Ozoguz, *Int. J. of Bif. and Chaos* **12** (2002) 23-42.
  8. Bocheng Bao, Guohua Zhou, Jianping Xu and Zhong Liu, *International Journal of Bifurcation and Chaos* **20** (2010) 2203-2211.
  9. A.S. Elwakil, S. Ozoguz and M.P. Kennedy, *International Journal of Bifurcation and Chaos* **13** (2003) 3093-3098.
  10. Guo-Qun Zhong, Kim-Fung Man and Guanrong Chen, *International Journal of Bifurcation and Chaos* **12** (2002) 2907-2915.
  11. Jinhu Lu and Guanrong Chen, *International Journal of Bifurcation and Chaos* **16** (2006) 775-858.
  12. C. Sánchez-López, E. Tlelo-Cuatle, M.A. Carrasco-Aguilar, F.E. Morales-López and B. Cante-Michcol, *Multi-scroll Chaotic Oscillator Employing UGCs*, International Conference on Electrical, Communications, and Computers, (2009).
  13. Kais Bouallegue, *Generation of Multi-Scroll Chaotic Attractors From Fractal and Multi-Fractal Processes*, Fourth International Workshop on Chaos-Fractals Theories and Applications, (2011).
  14. E. Campos-Cantón, J.G. Barajas Ramírez, G. Solís-Perales, R. Femat, *Chaos* **20** (2010) 013116.
  15. E. Campos-Cantón, R. Femat and G. Chen, *Chaos* **22** (2012) 033121.
  16. L.J. Ontanon-Garcia, E. Jimenez-Lopez, E. Campos-Cantón, and M. Basin, *Applied Mathematics and Computation* **233** (2014) 522-533.
  17. B.C. Bao, F.W. Hu, M. Chen, Q. Xu, and Y.J. Yu, *Int. J. Bifurcation Chaos* **25** (2015) 1550075.